

Development of an Enzyme-Inhibitor Reaction Using Cellular Retinoic Acid Binding Protein II for One-Pot Megamolecule Assembly

Blaise R. Kimmel^[b] and Milan Mrksich^{*[a]}

Abstract: This paper presents an enzyme building block for the assembly of megamolecules. The system is based on the inhibition of the human-derived cellular retinoic acid binding protein II (CRABP2) domain. We synthesized a synthetic retinoid bearing an arylfluorosulfate group, which uses sulfur fluoride exchange click chemistry to covalently inhibit CRABP2. We conjugated both the inhibitor and a fluorescein tag to an oligo(ethylene glycol) backbone and measured a second-order rate constant for the protein inhibition reaction

of approximately $3,600 \text{ M}^{-1}\text{s}^{-1}$. We used this new enzyme-inhibitor pair to assemble multi-protein structures in one-pot reactions using three orthogonal assembly chemistries to demonstrate exact control over the placement of protein domains within a single, homogeneous molecule. This work enables a new dimension of control over specificity, orientation, and stoichiometry of protein domains within atomically precise nanostructures.

Introduction

Megamolecules are very large protein structures that have molecular weights approaching 1 MDa and dimensions of 100 nm and are perfectly defined in the placement of each atom and bond.^[1,2] These structures are assembled through reactions of linkers that are terminally substituted with covalent inhibitors and fusion proteins containing enzyme targets for the inhibitors.^[3] A benefit of this approach is that initial binding of the inhibitor to the enzyme brings the partners together in a rapid reaction and activates the inhibitor only when it is at the site of desired reaction.^[4] Our previous work used the reaction of a cutinase protein with a *p*-nitrophenyl phosphonate (pNPP) and a SnapTag domain with a chloro-pyrimidine (CP) inhibitor to synthesize dendritic molecules,^[5] therapeutic antibody mimics,^[6] and to study structure-function relationships in antibody-enzyme conjugates (Figure 1A–B).^[7] The development of additional enzyme-inhibitor pairs will be important for enabling the efficient synthesis of complex protein architectures and possibly for preparing structures that are immunotolerant. In this work, we describe the development of an irreversible inhibitor for cellular retinoic acid binding protein II (CRABP2) and demonstrate its use in megamolecule assembly.

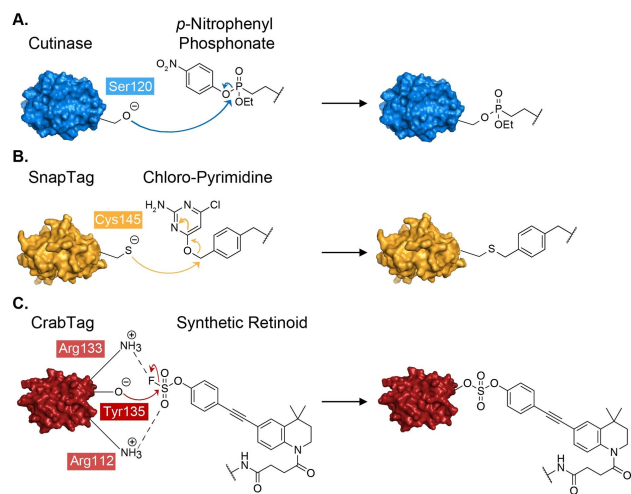


Figure 1. Reactions for assembly of megamolecules. Covalent inhibition of (A) cutinase with a *p*-nitrophenyl phosphonate (pNPP) inhibitor and of (B) SnapTag with a chloro-pyrimidine (CP) inhibitor. (C) In this work, covalent reaction of the CRABP2 (CrabTag) domain with a synthetic retinoid inhibitor.

Results and Discussion

Our design of the covalent inhibitor was based on a report by Kelly, Sharpless, and coworkers of covalent inhibition of CRABP2, at an active site tyrosine residue, by an arylfluorosulfate electrophile.^[8] This sulfur fluoride exchange (SuFEx) click reaction was activated by two proximal arginine residues (Arg112 and Arg133) that electrostatically stabilized the reactive sulfur fluoride bond through the formation of a sulfate ester, lowering the pK_a of the nucleophile and accelerating the inhibition reaction.^[8–11]

[a] Prof. M. Mrksich
Department of Biomedical Engineering, Department of Chemistry
Northwestern University
2145 Sheridan Road, Evanston, IL 60208 (USA)
E-mail: milan.mrksich@northwestern.edu

[b] B. R. Kimmel
Department of Chemical and Biological Engineering
Northwestern University
2145 Sheridan Road, Evanston, IL 60208 (USA)

Supporting information for this article is available on the WWW under <https://doi.org/10.1002/chem.202103059>

The rate of reaction with this inhibitor, however, was not well-suited for megamolecule assembly. Hence, we incorporated a synthetic retinoid described by Whiting, Pohl, and coworkers.^[12,13] The high affinity of this class of synthetic retinoids for CRABP2 owes to a highly-conjugated, linear backbone for binding into the hydrophobic ligand binding pocket of the protein.^[14] We prepared a synthetic retinoid with a modification at the hydrophobic region for ligation onto our linkers. The polar region of the retinoid displays the necessary arylfluorosulfate group for covalent modification by SuFEx with the monomeric CRABP2 active site tyrosine nucleophile (Figure 1C).

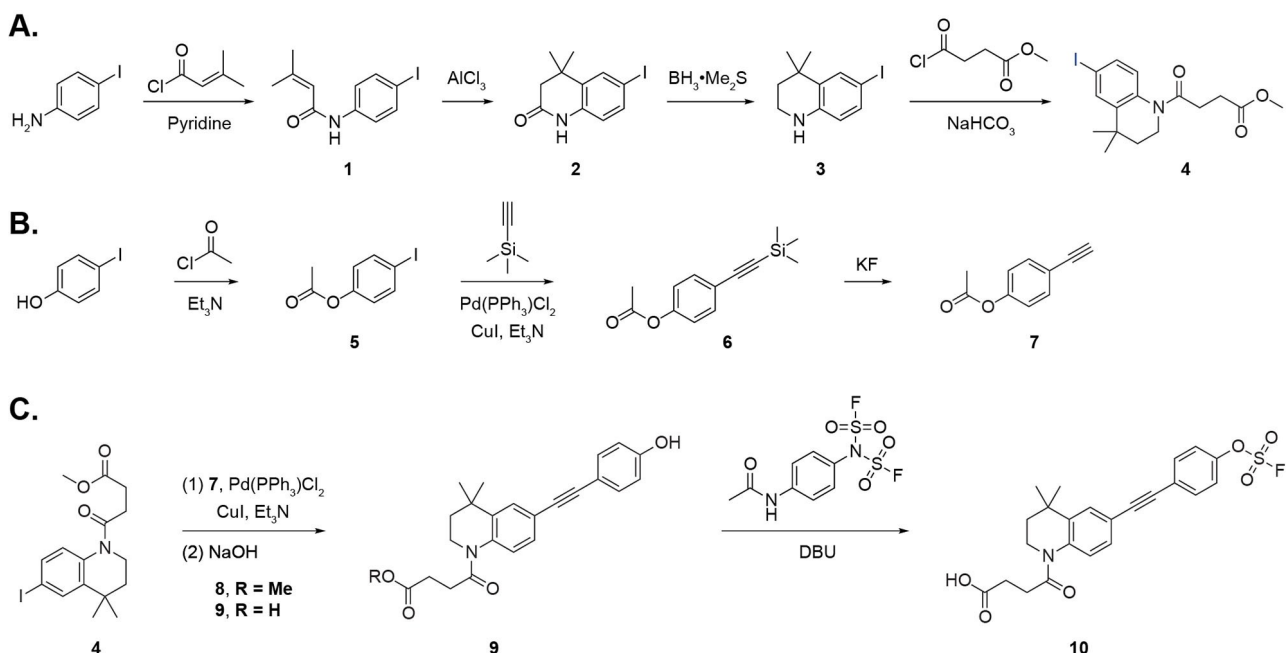
We prepared covalent inhibitor **10** in a 10-step convergent synthesis through the conjugation of π -donor **4** and π -acceptor **7** (Scheme 1). The former was synthesized from 4-iodoaniline by acylation (1) and Friedel-Crafts cyclization (2) followed by reduction with borane-dimethyl sulfide complex to yield tetrahydroquinoline **3**.^[15] Acylation with 4-chloro-4-oxobutyrate gave para-iodoaniline derivative **4**. The π -acceptor partner **7** was synthesized following an approach reported by Freccero.^[16] 4-Iodophenol was protected by O-acetylation (5), coupled to trimethylsilylacetylene by Sonogashira cross-coupling (6), and desilylated with potassium fluoride. The protected synthetic retinoid **8** was then conjugated through Sonogashira coupling of π -acceptor (**7**) and π -donor (**4**), followed by saponification to reveal non-covalent retinoid inhibitor **9** with a succinic acid handle for chemical ligation. We completed the synthesis by sulfonylation of the terminal phenol with [4-(acetylaminophenyl)imidodisulfuryl] difluoride (AISF) to give synthetic retinoid **10**.^[17]

We constructed a T7 expression plasmid incorporating the sequence for CRABP2 (referred to hereon as CrabTag) modified

with a C-terminal His-tag. We transformed the plasmid into chemically competent *E. coli* and purified the protein with immobilized metal affinity chromatography (IMAC).^[18] We reacted the protein (10 μ M) in phosphate buffered saline (PBS; 2.7 mM KCl, 138 mM NaCl, pH 7.4) with covalent inhibitor **10** (1.1 equivalents) and purified the adduct using size exclusion chromatography (SEC). Electrospray ionization mass spectrometry (ESI-MS) confirmed presence of the adduct (Figure S1–S2).

We grew crystals of the inhibited enzyme and obtained an X-ray structure that diffracted to 2.0 \AA ($R_{\text{work}} = 0.169$, $R_{\text{free}} = 0.228$) (PDBID: 7RY5) (Figure 2). The electron density map shows that the synthetic retinoid inhibitor forms a covalent sulfate ester adduct at the polar region of the inhibitor with the nucleophilic residue, Tyr135 (Figures S3–S6). A structural alignment comparison of the CRABP2 protein backbone in our CrabTag-**10** adduct with the non-covalent CRABP2-synthetic retinoid complex from Whiting and Pohl^[13] (PDBID: 6HKR) shows high similarity (RSMD = 1.18 \AA over all atoms without refinement) (Table S1). Consistent with the covalent CRABP2-diarylsulfate crystal structure from Sharpless and Kelly,^[8] synthetic retinoid inhibitor **10** selectively modifies Tyr135 polar stabilization interactions between the arylfluorosulfate electrophile. Further, the proximal hydrogen bonding donor (Arg112 and Arg133) side chains help to facilitate the covalent SuFEx modification of the Tyr135 residue.

We synthesized linker **11**, which included a fluorophore to characterize the kinetics for reaction of the covalent inhibitor and CrabTag (Figure 3A). We ran parallel reactions that varied the concentration of the linker (2, 5, 10, 20, 40, 65, and 100 μ M) at a constant concentration of CrabTag (1 μ M) and stopped the reactions using Laemmli reducing buffer at times ranging from 0 to 120 seconds (Figure 3B). Intact mass spectrometry analysis



Scheme 1. Synthesis of the CRABP2 synthetic retinoid covalent inhibitor. The synthesis is based on joining π -donor (**4**, A) with π -acceptor (**7**, B) followed by elaboration to give the covalent inhibitor (**10**, C). See text for details.

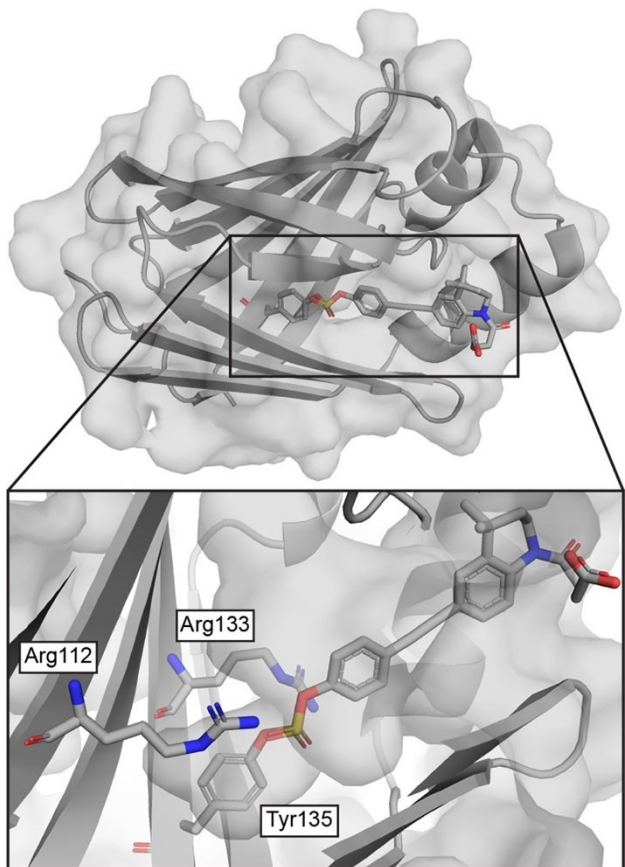


Figure 2. Crystal structure at 2.0 Å of the CrabTag-10 complex. Tyr135 forms a covalent bond with the arylfluorosulfate electrophile within synthetic retinoid inhibitor 10, where the resulting Tyr~Arg~Arg motif is specified. PDBID: 7RY5.

of the protein-inhibitor complexes for the reactions of CrabTag with either inhibitor **10** or **11** reveal monomeric adducts with only one modification that corresponds to the mass of either inhibitor (Figure 3C, Figure S2). We separated the reaction products with SDS-PAGE and quantitated the mean fluorescence intensity of protein bands that corresponded to the adduct with ImageJ. We fit the kinetic data to a single-phase exponential decay to obtain observed rate constants, k_{obs} (Figure 3D). We then plotted the k_{obs} values against the linker concentration to give a Michaelis-Menten curve, yielding the inactivation rate constant k_i and the equilibrium binding affinity of the enzyme-inhibitor complex K_i (Figure 3E). The ratio of these parameters gives the second order rate constant for the covalent modification reaction, k_{eff} , as $(3.6 \pm 0.5) \times 10^3 \text{ M}^{-1} \text{ s}^{-1}$. We also monitored the stability of the adduct by incubating the product (1 μM in PBS, 25 °C) and found that over 95% of the protein domains in solution retained covalent occupancy of the linker after two weeks (Figure S7).

We next demonstrate that we can assemble megamolecules using three reactions – CrabTag with **10**, cutinase with a pNPP inhibitor, and SnapTag with a CP inhibitor.^[2] Importantly, we first confirmed that each enzyme only reacts with its paired covalent inhibitor (see Supporting Information) and therefore

expected that branched megamolecule **16** could be assembled in a single, one-pot reaction from four reactants: cutinase, a SnapTag-CrabTag (SR) fusion protein, fluorescent linker **11**, and a heterotrifunctional linker bearing two inhibitors for SnapTag and one inhibitor for cutinase.^[5]

There are 120 discreet pathways that could give product **16**. Consideration of the relative rates for the reactions of the three enzymes narrows the possible pathways to the two shown in Figure 4A. Because the reaction of CrabTag with its inhibitor is the fastest, we expected that the SR fusion protein would first react with fluorescent linker **11** to give intermediate **12**. Based on the relative rates for SnapTag and cutinase reactions with their inhibitors, we expected that intermediate **13** would form next. In the next step, we predicted that two reaction pathways – forming either intermediates **14** or **15** – would compete to give final product **16**. After performing the experiment, we obtained time-resolved quantification of reaction intermediates and formation of final product **16** using both fluorescent and Coomassie stained SDS-PAGE (Figure 4B).

By monitoring the concentration of each intermediate, we can assess the kinetics and determine the abundance of each reaction intermediate over time (Figure 4C). We used the SimBiology application within MATLAB to develop a simple block diagram to model the batch reaction for the megamolecule assembly (Figure S12).^[19,20] Due to the fast reaction kinetics of CrabTag inhibition, a key assumption to our model was a pseudo-steady state hypothesis on the concentration of fluorescent linker **11**.^[21] Using a non-linear regression as our statistical model, we simultaneously solved the system of differential rate law equations and estimated the second-order kinetic rate constant parameters from the model (Figures S12–14, Tables S3–S6). This experiment revealed that a mechanistic approach could be used to describe and monitor the stepwise assembly of an atomically precise multi-protein scaffold over time.

We next synthesized heterotrifunctional linker **17** that bears a covalent inhibitor for each of the three enzyme-inhibitor pairs described in this work – SnapTag, cutinase, and CrabTag (see Supporting Information). Adding linker **17** (20 μM in PBS, 25 °C) into an equimolar solution of three monomeric enzymes (each at 22 μM) resulted in a one-pot reaction where only one copy of each enzyme was simultaneously and, importantly, site-selectively localized to the linker core to form branched megamolecule product **18** (Figure 5A). We purified the major reaction peak using SEC and compared homogeneous product **18** to the starting enzymes using SDS-PAGE and ESI-MS (Figure 5B–C). The exact molecular weight of branched megamolecule product **18** was 62,232 Da, which is in excellent agreement to the expected molecular weight of 62,231 Da ($\Delta\text{MW} = 1 \text{ Da}$). Further, TEM was used to image the structure for single-branched megamolecule structure **18** (FIGURE S15). The average structure length was measured for this product at 8 nm \pm 2 nm.

Finally, we describe the preparation of double-branched megamolecule **19** using heterotrifunctional linker **17** in a one-pot assembly involving six reactions of four molecules (Figure 5D). Assembly of megamolecule **19** was accomplished by reacting linker **17** (22 μM in PBS, 25 °C) with a mixture of both

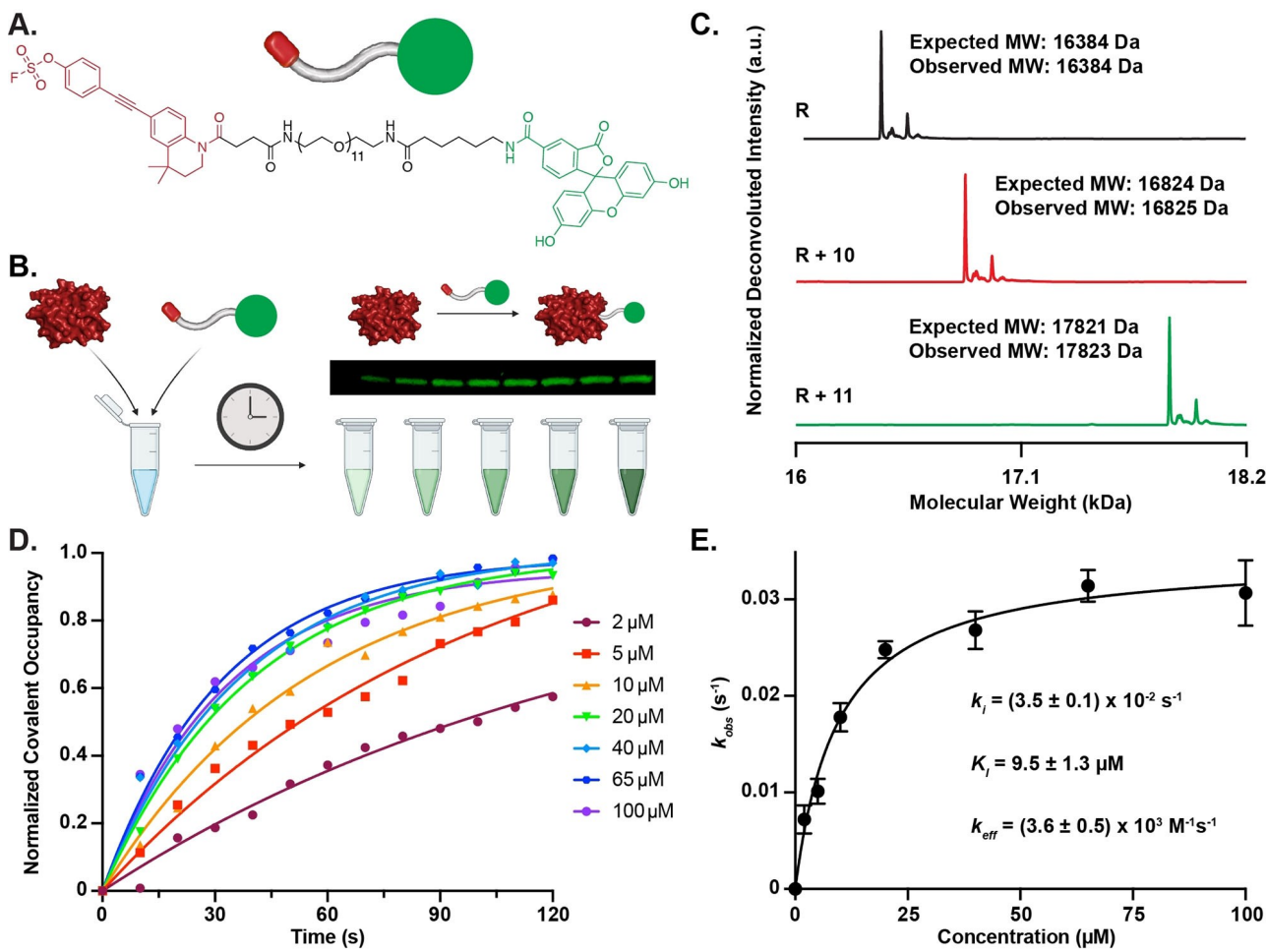


Figure 3. Kinetic characterization for the reaction of (A) synthetic retinoid inhibitor 11, which is terminated in a fluorescein tag (green). (B) Reaction of CrabTag with linker 11 was stopped at different time points using Laemmli buffer. Reaction products were separated using SDS-PAGE and the fluorescent product band was quantitated using ImageJ. (C) Deconvoluted protein mass spectrometry data quantifying the molecular weight of CrabTag (R, black) before and after complexation with either inhibitor 10 (red) or inhibitor 11 (green). (D) Fraction of covalently occupied CrabTag protein plotted for each linker concentration at discrete time points to give k_{obs} . (E) The k_{obs} data were plotted relative to the linker concentrations in a Michaelis-Menten analysis and gave constants k_i , K_i , k_{eff} . All plots and values have error represented as SEM. Figure was created using Biorender.com.

monomeric CrabTag and cutinase domains (both at 22 μM) and a di-SnapTag fusion protein (SS, 10 μM) core (Figure S11). Purification of product 19 by SDS-PAGE shows a product band near 120 kDa, which is consistent with the predicted molecular weight of approximately 124.5 kDa (Figure 5E). SEC was used to characterize each of the enzyme starting materials, single-branched product 18, and double-branched product 19. The calculated partition coefficients (K_{av}) for all proteins and megamolecules matched their expected molecular weights by alignment to the standard globular protein calibration curve (dotted line), indicating that each species had a single, globular structure (Figure 5F). TEM was finally used to image double-branched megamolecule 19, which had measured dimensions of $8 \text{ nm} \pm 2 \text{ nm}$ for the diameter and of $11 \text{ nm} \pm 3 \text{ nm}$ for the length (Figure S16). These results demonstrate the orthogonality of the enzyme-inhibitor reactions and their application to the one-pot assembly of complex products without the use of protecting groups.

Conclusions

This work establishes a new reaction pair for assembly of megamolecules. The CrabTag domain efficiently reacts with 10 due to the high affinity of the synthetic retinoid and the rapid covalent reaction of the arylfluorosulfate electrophile with the tyrosine nucleophile.^[8,12] The CrabTag protein domain is monomeric, easily expressed in *E. coli* due to its small size (17 kDa), and is also significant because it is a human-derived enzyme.^[8,22] Further, this inhibition reaction has an effective rate constant of approximately $3,600 \text{ M}^{-1}\text{s}^{-1}$ and the enzyme-inhibitor complex is stable ($>95\%$ bound) at room temperature for over two weeks. Finally, the orthogonality of this reaction relative to the other two enzyme-inhibitor reactions used here allowed us to perform single pot assemblies of complex products, demonstrating its utility for convergent megamolecule assembly. It is important to note that while the reactions between the inhibitors and the enzymes are rapid, the scale of megamole-

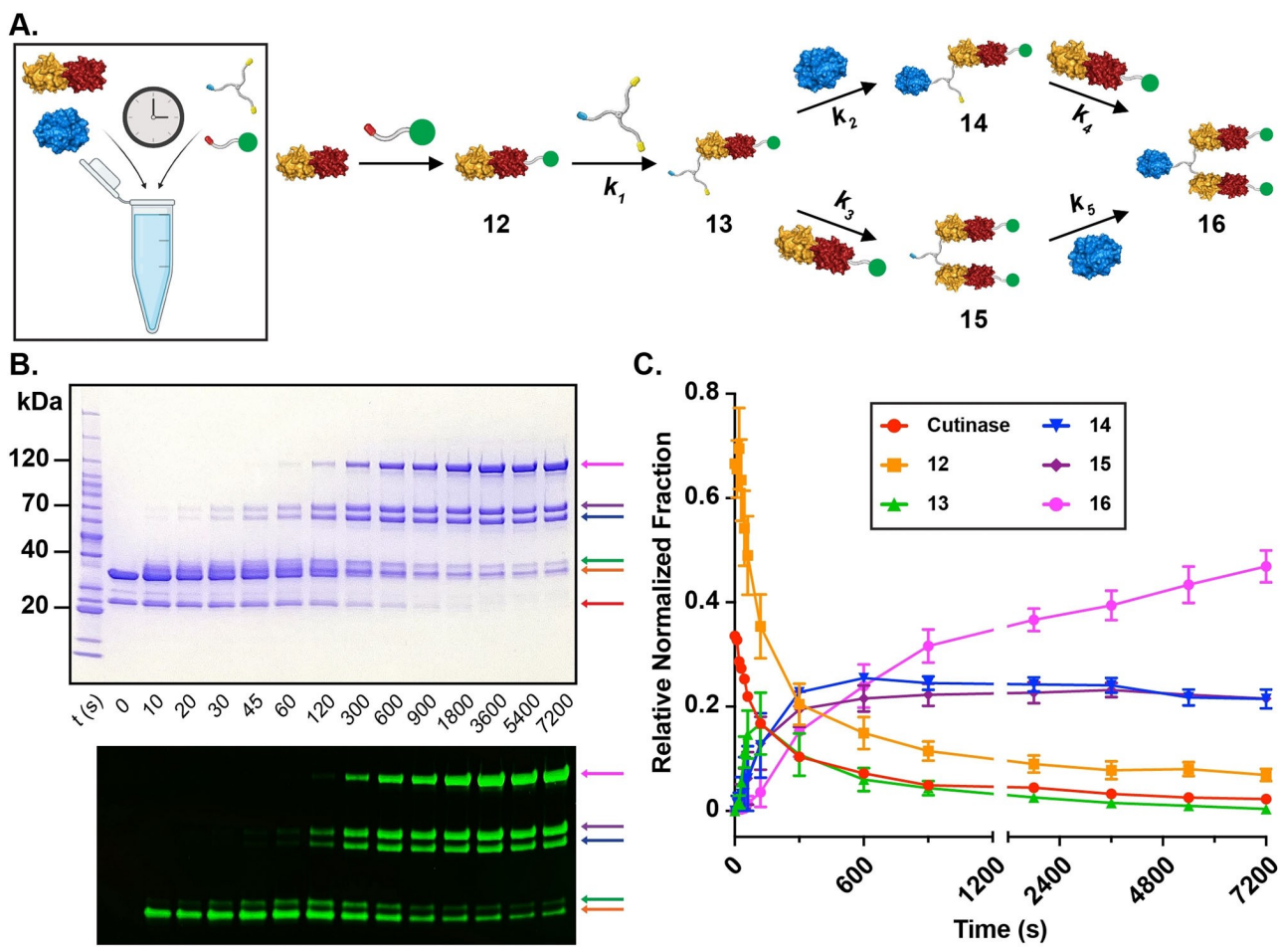


Figure 4. Monitoring one-pot megamolecule assembly. (A) Scheme of the one-pot multi-protein assembly synthesis from building blocks into product 16. (B) Top: Brightfield SDS-PAGE of the reaction over a two-hour time scale. Benchmark protein ladder for relative scale. Bottom: Fluorescent image of SDS-PAGE (Red arrow, Cutinase; Orange arrow, 12; Green arrow, 13; Blue arrow, 14; Purple arrow, 15; Magenta arrow, 16). (C) Plot showing the relative abundance of all reaction intermediates over time as quantified using both brightfield and fluorescent SDS-PAGE. Figure was created using Biorender.com.

olecule assembly is currently limited to several nanomoles of protein and linkers in one-pot.

We believe that this new reaction will play a significant role in the assembly of therapeutic antibody mimics,^[23] including antibody-drug conjugates,^[24,25] multi-specific antibodies,^[26,27] and hypervalent protein dendrimers.^[28,29] In each of these applications, it is critical that the assembly of several fragments results in a homogeneous target structure without the necessity for intermediate protecting and deprotecting reactions. Further, it will be important that the enzymes are human-derived to minimize unwanted immunogenicity.^[30–32] We expect that having a modular toolbox with the several, orthogonal enzyme-inhibitor reactions described in this work will enable efficient, one-pot assembly of a broad range of megamolecule architectures.

Acknowledgements

B.R.K. acknowledges support from the Ryan Fellowship, the International Institute for Nanotechnology at Northwestern

University, and the National Science Foundation Graduate Research Fellowship under Grant DGE-1842165. Research reported in this paper was supported by ARO MURI FA9550-16-1-0150. The authors thank Justin Modica and Bethel Shekour for help in collecting NMR spectra and Zhaoyi Gu in the purification of chemical linkers. The authors thank Valerie Tokars and Pamela Focia for performing TEM imaging and X-ray Crystallographic structure determination and refinement. This research used resources of the Advanced Photon Source; a U.S. Department of Energy (DOE) Office of Science User Facility operated for the DOE Office of Science by Argonne National Laboratory under Contract DE-AC02-06CH11357. Use of beamlines of the Life Sciences Collaborative Access Team (LS-CAT) located at Sector 21 of the APS was supported by the Michigan Economic Development Corporation and the Michigan Technology Tri-Corridor (Grant 085P1000817). This work also used resources of the Northwestern University Structural Biology Facility, which is supported by the NCI CCSG P30 CA060553 grant awarded to the Robert H. Lurie Comprehensive Cancer Center.

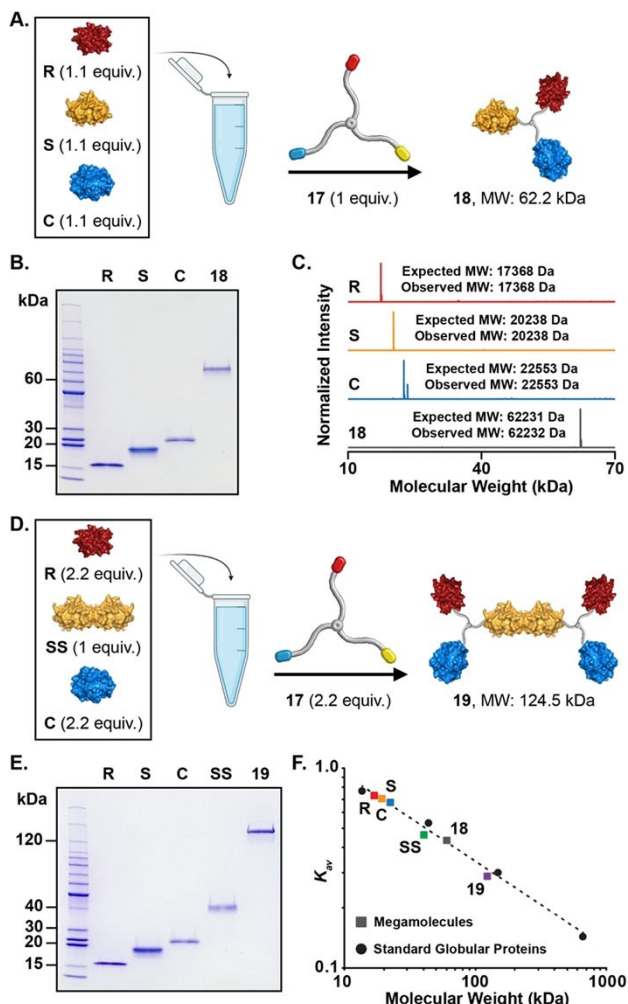


Figure 5. One-pot megamolecule reactions using heterotrifunctional linker 17. (A) Reaction Scheme depicting the one-pot synthesis of a megamolecule product 18. The core of the protein scaffold is trifunctional linker 17, which bears each of the three covalent inhibitors. (B) SDS-PAGE and (C) ESI-MS characterization of the enzyme reactants and purified one-pot megamolecule product 18. (D) One-pot reaction synthesis of double-branched megamolecule 19 using a di-SnapTag fusion protein as the scaffold core. (E) SDS-PAGE characterization of the starting proteins and product 19. (F) Analysis of partition coefficients (K_{av}) based on size-exclusion chromatograms from protein and megamolecule purification.

Conflict of Interest

The authors declare no conflict of interest.

Keywords: bioorganic chemistry • enzymes • inhibitors • kinetics • protein structures

[1] J. A. Modica, S. Skarpathiotis, M. Mrksich, *ChemBioChem* **2012**, *13*, 2331–2334.
 [2] J. A. Modica, Y. Lin, M. Mrksich, *J. Am. Chem. Soc.* **2018**, *140*, 6391–6399.

[3] E. L. Taylor, K. J. Metcalf, B. Carlotti, C. T. Lai, J. A. Modica, G. C. Schatz, M. Mrksich, T. Goodson, *J. Am. Chem. Soc.* **2018**, *140*, 15731–15743.
 [4] S. Zhou, K. J. Metcalf, P. Bugga, J. Grant, M. Mrksich, *ACS Appl. Mater. Interfaces* **2018**, *10*, 40452–40459.
 [5] B. R. Kimmel, J. A. Modica, K. Parker, V. Dravid, M. Mrksich, *J. Am. Chem. Soc.* **2020**, *142*, 4534–4538.
 [6] J. A. Modica, T. Iderzorig, M. Mrksich, *J. Am. Chem. Soc.* **2020**, *142*, 13657–13661.
 [7] K. J. Metcalf, B. R. Kimmel, D. J. Sykora, J. A. Modica, K. A. Parker, E. Berens, R. Dai, V. P. Dravid, Z. Werb, M. Mrksich, *Bioconjugate Chem.* **2021**, *32*, 143–152.
 [8] W. Chen, J. Dong, L. Plate, D. E. Mortenson, G. J. Brighty, S. Li, Y. Liu, A. Galmozzi, P. S. Lee, J. J. Hulce, B. F. Cravatt, E. Saez, E. T. Powers, I. A. Wilson, K. Barry Sharpless, J. W. Kelly, *J. Am. Chem. Soc.* **2016**, *138*, 7353–7364.
 [9] J. Dong, L. Krasnova, M. G. Finn, K. B. Sharpless, *Angew. Chem. Int. Ed.* **2014**, *53*, 9430–9448.
 [10] Q. Zheng, J. L. Woehl, S. Kitamura, D. Santos-Martins, C. J. Smedley, G. Li, S. Forli, J. E. Moses, D. W. Wolan, K. B. Sharpless, P. R. Chen, L. Wang, *Org. Lett.* **2021**, *23*, 4228–4232.
 [11] J. Han, J. Celaje, J. Thomas, V. Fokin, *FASEB J.* **2018**, *32*, 656.3–656.3.
 [12] V. B. Christie, J. H. Barnard, A. S. Batsanov, C. E. Bridgens, E. B. Cartmell, J. C. Collings, D. J. Maltman, C. P. F. Redfern, T. B. Marder, S. Przyborski, A. Whiting, *Org. Biomol. Chem.* **2008**, *6*, 3497–507.
 [13] D. R. Chisholm, C. W. E. Tomlinson, G. L. Zhou, C. Holden, V. Affleck, R. Lamb, K. Newling, P. Ashton, R. Valentine, C. Redfern, J. Erostýák, G. Makkai, C. A. Ambler, A. Whiting, E. Pohl, *ACS Chem. Biol.* **2019**, *14*, 369–377.
 [14] D. R. Chisholm, A. Whiting, *Meth. Enzymol.* **2020**, *637*, 453–491.
 [15] D. R. Chisholm, G.-L. Zhou, E. Pohl, R. Valentine, A. Whiting, *Beilstein J. Org. Chem.* **2016**, *12*, 1851–1862.
 [16] F. Doria, C. M. Gallati, M. Freccero, *Org. Biomol. Chem.* **2013**, *11*, 24.
 [17] H. Zhou, P. Mukherjee, R. Liu, E. Evrard, D. Wang, J. M. Humphrey, T. W. Butler, L. R. Hoth, J. B. Sperry, S. K. Sakata, C. J. Helal, C. W. Am Ende, *Org. Lett.* **2018**, *20*, 812–815.
 [18] J. A. Bornhorst, J. J. Falke, *Meth. Enzymol.* **2000**, *326*, 245–254.
 [19] A. David, K. G. Larsen, A. Legay, M. Mikucionis, D. B. Poulsen, S. Sedwards, A. David, K. G. Larsen, A. Legay, M. Mikucionis, B. D. Poulsen, *Int. J. Softw. Tools Technol. Transf.* **2015**, *17*, 351–367.
 [20] S. W. Smeal, M. A. Schmitt, R. R. Pereira, A. Prasad, J. D. Fisk, *Virology* **2017**, *500*, 259–274.
 [21] A. G. McDonald, K. F. Tipton, *eLS* **2020**, 1–17.
 [22] C. Schwaid, Adam. Discovery and Characterization of Novel Bioactive Peptides and a Natural ER α Ligand. **2013**.
 [23] A. R. Baloch, A. W. Baloch, B. J. Sutton, X. Zhang, *Crit. Rev. Biotechnol.* **2016**, 268–275.
 [24] S. C. Alley, N. M. Okeley, P. D. Senter, *Curr. Opin. Chem. Biol.* **2010**, 529–537.
 [25] J. R. McCombs, S. C. Owen, *AAPS J.* **2015**, *17*, 339–351.
 [26] J. B. Evans, B. A. Syed, *Nat. Rev. Drug Discovery* **2014**, *13*, 413–414.
 [27] C. T. Jiang, K. G. Chen, A. Liu, H. Huang, Y. N. Fan, D. K. Zhao, Q. N. Ye, H. B. Zhang, C. F. Xu, S. Shen, M. H. Xiong, J. Z. Du, X. Z. Yang, J. Wang, *Nat. Commun.* **2021**, *12*, 1359.
 [28] Y. Zhang, M. Üçüncü, A. Gambardella, A. Baibek, J. Geng, S. Zhang, J. Clavadetscher, I. Litzen, M. Bradley, A. Lilienkampf, *J. Am. Chem. Soc.* **2020**, *142*, 21615–21621.
 [29] F. J. Martinez-Veracoechea, D. Frenkel, *Proc. Natl. Acad. Sci. USA* **2011**, *108*, 10963–10968.
 [30] X. Zhang, X. Zhao, J. A. Luckanagul, J. Yan, Y. Nie, L. A. Lee, Q. Wang, *ACS Macro Lett.* **2017**, *6*, 442–446.
 [31] A. S. Pitek, S. A. Jameson, F. A. Veliz, S. Shukla, N. F. Steinmetz, *Biomaterials* **2016**, *89*, 89–97.
 [32] M. Ulitzka, S. Carrara, J. Grzeschik, H. Kornmann, B. Hock, H. Kolmar, *Protein Eng. Des. Sel.* **2020**, *33*, 1–12.

Manuscript received: August 22, 2021
 Accepted manuscript online: October 28, 2021
 Version of record online: November 17, 2021